HHS Public Access

Author manuscript

Curr Biol. Author manuscript; available in PMC 2024 April 10.

Published in final edited form as:

Curr Biol. 2023 April 10; 33(7): 1372–1380.e4. doi:10.1016/j.cub.2023.02.032.

Cross-modal modulation gates nociceptive inputs in *Drosophila*

Geng Pan[1], **Ruonan Li**[1,2], **Guozhong Xu**[3], **Shijun Weng**[3], **Xiong-li Yang**[3], **Limin Yang**[1,2,*], **Bing Ye**[1,4,*]

[1]Life Sciences Institute and Department of Cell and Developmental Biology, University of Michigan, Ann Arbor, MI 48109, USA

[2]School of Medicine, Dalian University, Dalian, Liaoning 116622, China

[3]Institutes of Brain Science, Fudan University, Shanghai 200032, China

[4]Lead contact

SUMMARY

Animals' response to a stimulus in one sensory modality is usually influenced by other modalities[1]. One important type of multisensory integration is the cross-modal modulation, in which one sensory modality modulates (typically inhibits) another. Identification of the mechanisms underlying cross-modal modulations is crucial for understanding how sensory inputs shape animals' perception and for understanding sensory processing disorders[2-4]. However, the synaptic and circuit mechanisms that underlie cross-modal modulation are poorly understood. This is due to the difficulty of separating cross-modal modulation from multisensory integrations in neurons that receive *excitatory* inputs from two or more sensory modalities[5] – in which case it is unclear what the modulating or modulated modality is. In this study, we report a unique system for studying cross-modal modulation by taking advantage of the genetic resources in *Drosophila*. We show that gentle mechanical stimuli inhibit nociceptive responses in *Drosophila* larvae. Low-threshold mechanosensory neurons inhibit a key second-order neuron in the nociceptive pathway through metabotropic GABA receptors on nociceptor synaptic terminals. Strikingly, this cross-modal inhibition is only effective when nociceptor inputs are weak, thus serving as a gating mechanism for filtering out weak nociceptive inputs. Our findings unveil a novel cross-modal gating mechanism for sensory pathways.

Graphical Abstract

[*]**Correspondence**: Bing Ye (bingye@umich.edu); Limin Yang (yanglimin@dlu.edu.cn). **Tweeter handle**: @byneuron.

AUTHOR CONTRIBUTIONS

G.P., L.Y., and B.Y. conceived the project and designed the experiments. G.P. participated in all experiments and analyzed the data. R.L., and L.Y. participated in part of the electrophysiological experiments. G.X., S.W., and X-L.Y. assisted in establishing the patch-clamping recording of larval neurons. B.Y. supervised the project. G.P. and B.Y. wrote the paper.

DECLARATION OF INTERESTS

The authors declare no competing interests.

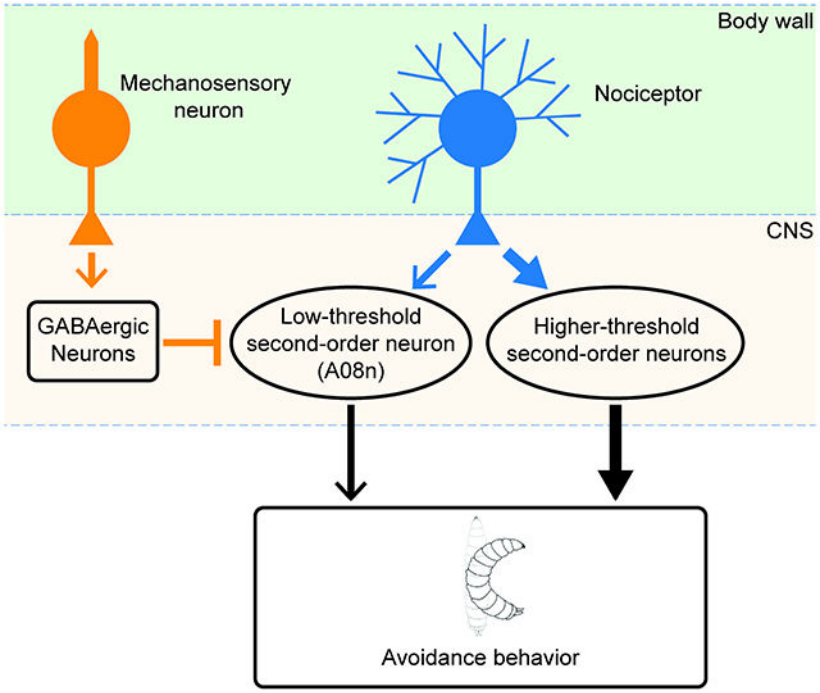

eTOC Blurb

Pan et al. show that gentle mechanical stimuli inhibit nociceptive responses in *Drosophila* larvae. Due to the inhibition of a second-order neuron that responds to weak nociceptor inputs, this cross-modal inhibition is only effective when noxious cues are weak, thus serving as a mechanism to filter out weak nociceptive inputs.

Keywords

cross-modal modulation; multisensory integration; nociceptive behavior; sensory gating; GABAergic modulation; presynaptic inhibition; *Drosophila*

RESULTS

Mechanosensory inputs through the chordotonal neurons inhibit the nociceptive pathway

The somatosensory system of the *Drosophila* larva has recently emerged as an effective model for discovering the principles of sensory circuit function, plasticity, and assembly. *Drosophila* larvae respond to noxious stimuli or nociceptor stimulation by curling their bodies and then rolling around their rostro-caudal axis[6,7]. The class IV dendritic arborization (C4da) neurons on the larval body wall, are polymodal nociceptors[7-9], whereas the chordotonal (Cho) and the class III dendritic arborization (C3da) neurons are low-threshold mechanosensory neurons[10-12]. The dendrites of these neurons are on the body wall, while their axon terminals (i.e., presynaptic terminals) are in the ventral nerve cord (VNC). *Drosophila* larvae escape from noxious heat[6,7]. To assess how low-threshold mechanosensory neurons affect the nociceptive responses, we tested the behavioral response of larvae to heat while inhibiting the Cho mechanosensory neurons optogenetically through

Guillardia theta anion channelrhodopsin-1 (GtACR1)[13,14]. The probability of larval escape behaviors exhibit a sigmoid relationship to linearly scaled temperatures[15]. Based on larvae's behavioral response to different temperatures[15], we examined the effect of inhibiting mechanosensory neurons on their nociceptive response to a low (27.5°C) and a high (39°C) temperature. Intriguingly, inhibition of the Cho neurons increased the nociceptive rolling of larvae by 131 % at 27.5°C but had no effect at 39°C (Figure 1A). This result suggests that Cho mechanosensory neurons inhibit the nociceptive pathway when the noxious stimulus is weak.

To confirm that mechanosensory neurons modulate the behavior elicited by nociceptor activation, we specifically activated the C4da nociceptors optogenetically via channelrhodopsin-2^{T195C} (ChR2^{T195C}; 470-nm light)[16] while inhibiting Cho neurons optogenetically with GtACR1 (617-nm light)[13,14]. Inhibition of the Cho neurons led to a 96% increase in the probability of nociceptive rolling (Figure 1B), while inhibition of the C3da neurons—another type of low-threshold mechanosensory neurons—did not change nociceptor-elicited rolling. Moreover, inhibition of Cho neurons shifted the stimulus-response curve of the rolling behavior to a more sensitive range (Figure 1C), suggesting that larvae are more sensitive to nociceptor activation when Cho neurons are inhibited. As a control, blue light (470-nm) did not elicit any rolling at a much stronger intensity (300 μW/mm^2) in larvae (C4da>ChR2^{T195C}) raised on food without all-trans-retinal (ATR) (n = 119), which is essential for activating the neurons via ChR2^{T195C}.

Mechanosensory neurons inhibit the nociceptor-specific second-order neuron A08n to modulate nociceptive behavior

The C4da nociceptors synapse on a variety of second-order neurons (SONs), including A08n, Basin4, Wave, mCSI, and DnB neurons[12,17-22]. These SONs, except A08n[18], also receive direct, excitatory inputs from the Cho and/or C3da mechanosensory neurons and are thus multisensory neurons (Figure 1D). The multisensory SONs' responses to concurrent stimulations of nociceptors and mechanosensory neurons are additive or superadditive[12,17,19,21].

We investigated how SONs respond to the combined activation of nociceptors and low-threshold mechanosensory neurons by performing whole-cell patch-clamp recordings of SONs in a larval preparation with intact PNS and CNS[15,18] (Figure 1E). The C4da nociceptors were activated optogenetically through ChR2^{T195C}, and gentle touches were applied to the larval body wall with a piezoelectric actuator. By calcium imaging of Cho axon terminals, we confirmed that such gentle touches activated Cho (Figure S1A-B), which is consistent with previous reports based on Ca^{2+} imaging of Cho somas[23]. Evans blue staining[24] suggests that touch stimuli did not damage the tissues on the body wall (Figure S1C-D).

While Basin-4 and Wave neurons responded to nociceptor activation with a single graded membrane depolarization, A08n responded by a train of spikes on top of a graded depolarization (Figure 1E)[15]. Current injection experiments confirmed that A08n is a spiking neuron while Basin-4 and Wave are not (data not shown). Considering that the amplitudes of A08n's responses are small and that some of the spikes may not be action

potentials, we use the term “spikelets” to describe these responses. Spikelets are brief, spike-like depolarizations of small amplitudes (typically smaller than 20 mV)[25,26].

Consistent with the notion that A08n does not receive direct inputs from mechanosensory neurons[18], they did not respond to gentle touches (Figure S2B-C). However, gentle touches suppressed the number of spikelets in A08n’s response to optogenetic activation of nociceptors (Figure 1E) without affecting the depolarization amplitude (Figure S2C). By contrast, gentle touches enhanced the responses of Basin-4 and Wave to nociceptor activation, which is consistent with the notion that these two neurons are multisensory SONs that receive excitatory inputs from both mechanosensory neurons and nociceptors[12,19]. Blue light (470-nm) alone did not activate A08n (Figure S2D-E). The A08n neurons thus offers an opportunity for studying the synaptic and circuit mechanisms underlying cross-modal inhibition with clearly defined modulating and modulated inputs.

We further found that Cho’s inhibition of larval behavioral responses to nociceptor stimulation requires active A08n neurons. Consistent with previous reports[15,18,27], optogenetic inhibition of A08n neurons with GtACR1 greatly reduced nociceptive rolling induced by C4da activation (Figure 1F). Importantly, inhibition of A08n abolished the increased rolling caused by inhibiting Cho neurons, which suggests that the mechanosensory-to-nociceptive cross-modal modulation requires the activation of A08n neurons.

Taken together, these results suggest that low-threshold mechanosensory neurons suppress nociceptive behavior by inhibiting the nociceptor-specific SONs that operate at low-intensity of nociceptor activation.

Cho neurons selectively suppress weak inputs from nociceptors

Cho mechanosensory neurons inhibit the nociceptive behavioral responses only when the noxious stimulus is weak (Figure 1A). Moreover, we previously found that among the SONs postsynaptic to C4da nociceptor, A08n is the most sensitive to nociceptor activation[15]. These findings prompted us to examine the effects of gentle touch on different levels of nociceptor activation. C4da nociceptors were optogenetically activated by different intensities of 470-nm light, while a gentle touch was applied to the body wall by a piezoelectric actuator. Intriguingly, we found that the inhibition of A08n’s response to nociceptor activation depended on the nociceptor’s activity level. A08n neuronal response was inhibited more at the low levels of C4da activation (0.40-1.04 μW/mm^2, 470-nm) (Figure 2A). The inhibitory effect by touch disappeared when nociceptors were activated by 1.5 μW/mm^2 of light. This result suggests that the cross-modal modulation suppresses the weak inputs from the C4da nociceptors.

Consistent with its role in the cross-modal modulation of nociceptive behavioral responses, activation of the Cho mechanosensory neurons led to inhibition of nociceptor-elicited A08n responses. Due to the fact that the blue light activating ChR2^{T195C} also activates the red-shift CsChrimson[28], we could not activate the nociceptors at different intensities while activating low-threshold mechanosensory neurons. We thus resorted to a chemogenetic approach for stimulating mechanosensory neurons while optogenetically activating nociceptors at various

intensities. The human adenosine-triphosphate (ATP)-gated cation channels formed by $P2X_2$ subunits[18,29] was expressed specifically in either Cho or C3da mechanosensory neurons, both of which share multisensory SONs with nociceptors. Perfusion of ATP activates these channels and thus the targeted neurons. Activation of Cho neurons by either a lower (0.33 mM) or a higher (1 mM) concentration of ATP inhibited nociceptor-elicited A08n responses at lower levels of nociceptor activation (0.39-2.31 $\mu W/mm^2$) but not at higher levels of nociceptor activation (Figure 2B). By contrast, activation of C3da mechanosensory neurons did not inhibit nociceptor-elicited A08n responses (Figure 2C). These results suggest that Cho neurons selectively suppress the weak inputs from the C4da nociceptors.

Strikingly, optogenetic inhibition of the Cho neurons via GtACR1 dramatically increased the nociceptor-elicited A08n responses at low, but not high, levels of nociceptor activation (Figure 2D). These results suggest that basal activities of Cho mechanosensory neurons gate the weak inputs from the C4da nociceptors.

Taken together, the results from our behavioral (Figure 1) and electrophysiological (Figure 2) experiments show that the Cho mechanosensory neurons selectively suppress weak inputs from nociceptors.

The cross-modal gating of nociceptive inputs is mediated by $GABA_B$ receptors in nociceptors

As in vertebrates, GABAergic modulation is the major type of synaptic inhibition in *Drosophila*[30]. We thus tested the possibility that the cross-modal gating of nociceptive inputs by Cho mechanosensory neurons is mediated by GABAergic signaling. Receptors of the neurotransmitter GABA include ionotropic $GABA_A$ and metabotropic $GABA_B$ types. We blocked these two types of receptors with their respective antagonist, and recorded nociceptor-elicited responses in A08n in the presence or absence of touch. CGP54626, an antagonist for $GABA_B$ metabotropic receptors[31], eliminated the cross-modal inhibition of nociceptor-elicited responses by touch (Figure 3A). By contrast, the GABA-gated Cl^- channel blocker picrotoxin (PTX)[32] had no effect on this cross-modal inhibition. Consistent with the finding 1 that Cho inhibition increased A08n responses at low—but not high—levels of nociceptor activation (Figure 2D), CGP54626 reversed the inhibition of A08n responses by Cho activation preferentially when nociceptors were activated at low levels (Figure 3B). These results suggest that $GABA_B$ receptors mediate the cross-modal gating of nociceptive inputs by Cho mechanosensory neurons.

We further identified the $GABA_B$ receptor involved in this cross-modal gating. Using a MiMIC-RMCE line ($GABA_BR1$-GFSTF) which fuses enhanced green fluorescence protein (EGFP) to the endogenous $GABA_BR1$[33], we found that the $GABA_BR1$ receptor was located in the vicinity of the axon terminals of C4da nociceptors in the VNC (Figure 3C). We then knocked down *$GABA_BR1$* specifically in the C4da nociceptors with transgenic small hairpin RNAs (shRNAs)[34] against this gene and examined the effects on the cross-modal inhibition of nociceptive inputs by mechanosensory neurons. Two different shRNA transgenes against $GABA_BR1$ ($shRNA^{BL51817}$ and $shRNA^{BL28353}$) both reversed the inhibition of A08n responses (Figure 3D). Moreover, knockdown of $GABA_BR1$ increased larval rolling elicited by nociceptor activation (Figure S3), similar to the effect of inhibiting Cho neurons (Figure

1B). Furthermore, whereas activation of Cho neurons suppressed C4da-induced nociceptive rolling, this effect was abolished by the knockdown of $GABA_BR1$ receptors in C4da nociceptors (Figure 4A).

Taken together, these results suggest that the Cho mechanosensory neurons inhibit low-threshold SONs (A08n) by GABAergic inhibition of nociceptor synaptic outputs and consequently suppresses larvae's behavioral response to weak inputs from nociceptors (Figure 4B).

Nociceptor-elicited body movements attenuate nociceptive inputs

Consistent with previous findings that peristaltic muscle contractions activate Cho neurons in dissected *Drosophila* larvae[35], we found that the peristaltic body movements—which are typically exhibited in crawling—activate these neurons in larvae that were not dissected (Figure S4A-B and Video S1). In light of our finding that Cho neurons inhibit the nociceptive pathway, we were curious how changes in Cho activity affect larvae's crawling elicited by nociceptive stimulations. Larvae's behavioral responses to nociceptor stimulation depend on the surface that they are on. In order to examine the effect of crawling, we minimized larval rolling by placing them on dry surfaces because a thin layer of water is required for assaying the nociceptive rolling[6]. Moreover, to minimize larva's digging into soft agar upon nociceptor activation, we placed them on hard agar (2%). Under such a condition, larva's primary response to nociceptor stimulation is crawling (Figure 4C).

Larvae tested in this "dry hard-agar assay" expressed $ChR2^{T159C}$ in their C4da nociceptors and either GtACR1 or mCD8-GFP (as a negative control for GtACR1) in their Cho mechanosensory neurons. $ChR2^{T159C}$ and GtACR1 were activated by 470-nm (16 μW/mm^2) and 617-nm (55 μW/mm^2) light, respectively. Larval behavior were analyzed with the software LabGym[36]. We found that inhibition of Cho neurons increased the speed of nociceptor-elicited crawling in the first second of nociceptor stimulation (Figure 4D). Inhibition of Cho did not affect the speed of crawling in the absence of nociceptor stimulation.

Taken together, these results suggest that nociceptor-elicited body movements attenuate nociceptive inputs in *Drosophila* larvae.

DISCUSSION

In scenarios where multisensory integration shows clear separation of the modulating and modulated sensory modalities, it is conceivable that the intensity of the *modulating* signal influences the effect of the cross-modal modulation. By contrast, the present study exemplifies an input-dependent cross-modal modulation. The fact that A08n neurons do not receive excitatory inputs from Cho mechanosensory neurons[18] but are instead inhibited by these mechanosensory neurons allowed us to test whether the intensity of the modulated modality—nociception in this case—has an impact on the cross-modal modulation. Among the tested SONs postsynaptic to C4da nociceptor (Basin4, Wave, mCSI, DnB, and A08n), A08n is the most sensitive to nociceptor activation[15]. Weak stimulation of nociceptors preferentially activates A08n. As a result, the only known SON that operates at low-intensity

of nociceptor activation is A08n. It thus makes sense for the intensity-dependent filter to act on this SON.

Unlike A08n, other SONs are multisensory neurons that receive excitatory inputs directly from the Cho mechanosensory neurons[12,17,19,21]. They serve to integrate the converged nociceptive and gentle mechanosensory inputs and respond to the two excitatory inputs additively or super-additively. This may cancel out the GABAergic inhibition at high levels of nociceptor activation. In fact, a prior work has suggested that Cho neurons facilitate the nociceptive behavior through the Basin neurons[12].

A number of studies found that the interactions between excitatory and inhibitory systems modulate nociception and pain in mammals, supporting the gate control theory of pain[37,38]. The gating of afferent fibers (e.g., Aβ) from contributing to pain in the gate control theory is different from our finding of gating through cross-modal inhibition. We found that when nociceptive inputs are weak, mechanosensory inputs suppress the nociceptive pathway, rather than contribute to it as in mammalian spinal cord. Moreover, this cross-modal gating is only effective on weak nociceptive inputs and thus serves as a filter that blocks low-intensity nociceptive inputs. Future work will determine whether this mechanism is also employed in vertebrate nociceptive or other sensory systems.

Little is known about the CNS mechanisms that gate nociceptive signals in *Drosophila*. The present study shows a gating mechanism mediated by GABAergic signaling. The identity of the GABAergic neurons mediating this modulation remains a mystery. This is a challenging issue to address. The GABAergic neurons postsynaptic to Cho neurons form complex networks, including both feedforward and recurrent circuits[39], which complicates the experiments involving the manipulations of these neurons. In fact, we tested several candidate neurons, including Drunken-1/2, LN-Hb and Griddle-2[39], but saw little effect on the cross-modal modulation. These might suggest that these neurons are not involved but might also be due to redundancy or recurrent GABAergic networks. Moreover, such studies are restricted by the availability of driver lines for transgene expression in the GABAergic neurons. Nevertheless, this is an important topic for future studies.

In their living environment, larval Cho neurons are stimulated by several types of mechanical cues. Besides touch, Cho neurons are known to be activated by sound and body movements and thus serve as sound-sensing neurons and proprioceptors[10,12,23,40,41]. In addition to these mechanical cues, larvae also encounter a variety of noxious cues in their living environment, including pokes from predators[7], noxious chemicals[42], and ultraviolet irradiations[43], which elicit dramatic avoidance responses of the larvae. While these avoidance behaviors are beneficial for larvae to escape from harm, excessive responses to low-intensity (and thus less harmful) noxious cues would diminish their ability to escape effectively (e.g., the ability of digging into a substrate to avoid further harms) and affect their activities for survival (e.g., foraging). We previously showed that nociceptor activation during development reduces the synaptic transmission from nociceptors to their SONs[18], demonstrating a mechanism through which larvae adjust their behavioral response to the chronic presence of noxious cues. In the present study, we show that gentle mechanosensory inputs selectively inhibit low-intensity nociceptive inputs. Cho activity modulates larvae's

behavior elicited by nociceptor stimulation. Consistent with previous findings that peristaltic muscle contractions activate Cho neurons[35], we found that larval body movement activate these neurons. Activation of nociceptors increases larval body movements. When the larvae's Cho mechanosensory neurons are inhibited, these body movements are increased. There are two conceivable reasons why larvae's nociceptor-elicited movements are regulated by Cho activity. It is possible that once these innate responses to noxious stimuli starts, the increased mechanosensory input dampens the nociceptive inputs, encouraging the larvae to increase these movements. It is also possible that the modulation of nociceptive inputs by mechanosensory inputs regulates the larva's perception of the noxious cue and thus the need of initiating the innate responses. Advanced approaches need to be developed in order to distinguish these two possibilities which requires determining the "motivation" of the larvae.

In summary, we show that cross-modal inhibition serves as a filter to block weak inputs but allow strong inputs to pass. One of the functions of this filter is to attenuate low-intensity nociceptive inputs through mechanosensory inputs, which would allow the animal to prioritize behaviors that are more important. Our findings unveil a novel cross-modal gating mechanism for sensory pathways.

STAR METHORDS

RESOURCE AVAILABILITY

Lead Contact—Further information and requests for resources and reagents should be directed to and will be fulfilled by the lead contact, Bing Ye (bingye@umich.edu).

Materials Availability—This study did not generate new unique reagents.

Data and Code Availability

- This study did not generate any datasets of standardized datatypes. All the data reported in this paper will be shared by the lead contact upon request.
- This study did not generate any original code.
- Any additional information required to reanalyze the data reported in this paper is available from the lead contact upon request.

EXPERIMENTAL MODEL AND SUBJECT DETAILS

Foraging 3rd-instar larvae were used. All experiments were done on age- and size-matched larvae. The fly stocks used in this study are in KEY RESOURCES TABLE.

METHOD DETAILS

Behavioral tests—*Drosophila* larvae were cultured in food containing 1 mM all-trans-retinal (ATR) (A.G. Scientific). ChR2^{T159C} was expressed in C4da nociceptors with *ppk*-GAL4 and UAS-ChR2^{T159C} or TrpA1-QF and QUAS-ChR2^{T159C} transgenes[15,18]. Inhibition of Cho was done with larvae carrying the *iav*-GALA and UAS-GtACR1 transgenes, and that of C3da neurons was done with larvae carrying the GMR83B04-GAL4[44] and UAS-GtACR1 transgenes[14]. During the test, larvae were placed on a Ø35 mm petri dish containing a

thin layer of water. Except the test of different intensities of 470-nm light in Figure 1C, 16 μW/mm^2 of 470-nm light was applied to activate ChR2^{T159C}. The intensity of 617-nm light was 55 μW/mm^2 for all experiments. Unless noted otherwise, the duration of 470-nm light application for all behavioral tests was 5 sec. GtACR1 currents reach the plateau in 200-300 ms[45], while ChR2 currents reach the peak in a few milliseconds[46,47]; to ensure the optogenetic inhibition of neuronal activity, 617-nm light was applied to activate GtACR1 250 ms earlier than the 470-nm light for activating ChR2^{T159C}. Larvae's response were recorded by a webcam (C910, Logitech, USA). Rolling was defined as ≥ 360° body rolls around the rostrocaudal axis[7]. Rolling probability is defined as the percentage of larvae that rolled during the defined period (5 sec for optogenetic stimuli and 1 min for heatplate) immediately after the stimulus started. All LEDs used were from LUXEON StarLED. Light intensity was measured with a power meter (PM16-122, Thorlabs, USA). Lights were controlled by a microcontroller board (Arduino UNO, Arduino).

To test larvae's behavioral response to heat, we used a heat-plate system consisting of a plate device that provides fast direct-contact temperature changes up to 70°C (CP-031, TE technology, USA), a temperature controller (TC-720, TE technology, USA), and a 12 V power supply (PS-12-8.4A, TE technology, USA)[48]. A black aluminum plate (1 mm thick) was glued to the top of the temperature controlling system (with double-sided thermally conductive tapes) to provide a dark background for the behavioral test. In addition, the edge of aluminum plate was wrapped with foam, and a thin layer of water—which is necessary for larvae to perform rolling[6] was kept on the surface of the plate during test. Larvae started to roll at ~27.5°C and the rolling probability reaches the plateau at ~40°C[15]. Thus, 27.5°C and 39°C were selected as low and high temperatures for noxious stimulations, respectively. Larvae expressing GtACR1 in their Cho neurons (*iav*-GAL4/UAS-GtACR1) were reared in food containing 1 mM all-trans-retinal (ATR), which is required for GtACR1 activation. Larvae reared on food without ATR were used as negative control for GtACR1 activation. After the heat plate reached the desired temperature, larvae were placed on the heat plate and illuminated with 617-nm light at 55 μW/mm^2. Larval rolling that occurred within 1 min after the larvae were placed on the heat plate were counted.

For the hard-agar assay, 2% agar was used to provide a hard substrate for larvae to crawl, and the surface was dry. On such a substrate, larvae rarely rolled or dug in response to nociceptor stimulation but crawled fast. ChR2^{T159C} was expressed in the C4da nociceptors, and either GtACR1 or mCD8-GFP was expressed in the Cho neurons. Larvae were raised on food containing 1 mM ATR. Third-instar larvae were placed on the agar plate and illuminated with 470-nm (16 μW/mm^2) and 617-nm (55 μW/mm^2) lights for 2 sec. The response of larvae were recorded with a webcam (C910, Logitech, USA) and analyzed with the software LabGym (v1.4)[36]. Crawling speed was calculated as the speed (pixels of displacement per sec) normalized to the size of the larva in pixels. 0.5 sec was used as the time window for speed measurement in LabGym (v1.4), so each data-point in Figure 4D shows the speed in the prior 0.5 sec.

Whole-cell patch-clamp recordings—The recordings were performed on a larval preparation with intact PNS and CNS[15,18]. After the larva was opened up by making a cut along its dorsal midline, the four corners of the body wall were pinned down with

the tissue side facing up on a chamber coated with sylgard. A small cut was made on one side of the VNC with a fine-tip glass needle to expose the SONs expressing mCherry for patch-clamp recording. The recording pipettes (4-6 MΩ) were made with borosilicate glass (Sutter, Novato, CA). The internal solution contained: 140 mM K-Gluconate, 10 mM HEPES, 4 mM MgATP, 0.5 mM Na_3GTP, 1 mM Na_4EGTA, and 1 mM KCl (pH 7.2; ~265 mOsm). The larva was perfused with the bath solution (~1 mL/min) containing: 103 mM NaCl, 3 mM KCl, 8 mM Trehalose, 26 mM $NaHCO_3$, 5 mM TES, 1 mM NaH_2PO_4, 1.5 mM $CaCl_2$, 4 mM $MgCl_2$, 10 mM glucose and 1 mM Na-L-glutamate (pH 7.3; 270-275 mOsm). Recordings were performed at room temperature (23-25°C). Current-clamp recordings were filtered at 3 kHz and digitized at 10 kHz. Signals were acquired by a Digidata 1550B digitizer and MultiClamp 700B amplifier (Molecular Devices).

During electrophysiological recordings, 470-nm and 560-nm light from LEDs were used to activate $ChR2^{T159C}$ and GtACR1, respectively. The LEDs were collimated into the light path of the microscope (BX51WI, Olympus, Japan), and controlled with light source control module (BioLED BLS, Mightex, USA). For brief optogenetic activations of C4da nociceptors, 50 ms of 470-nm light was applied, and SONs' responses within a 100-ms time-window from the onset of the activation were analyzed. For prolonged activations of 500-ms durations, A08n responses during the entire period were analyzed. For optogenetic inhibition via GtACR1, the intensity of 560-nm was 7.8 μW/mm^2, which did not lead to A08n response in the larvae expressing $ChR2^{T194C}$ in their C4da nociceptors. The resting time between each stimulation was ≥ 30 sec. For the reason explained in *Behavioral tests*, to ensure the optogenetic inhibition of neuronal activity, 560-nm light was applied to activate GtACR1 250 ms earlier than the 470-nm light for activating $ChR2^{T159C}$.

Touch stimuli were applied to the abdominal segment 4-6 (A4-A6) segments of the larval body wall with a piezoelectric actuator (PK2FVF1, Thorlabs, USA) controlled by a Piezo controller (KPZ101, Thorlabs, USA). Touch pipettes with rounded tips (Ø ~30 μm) were prepared with a pipette puller (P-97, Sutter instrument, USA). Using patch-clamp recordings, we found that SON responses to touches were delayed by over 70 ms. By contrast, their responses to optogenetic stimulations of sensory neurons were almost instantaneous. Possible causes of the extended delay in touch-elicited responses include the mechanical deformation of the body wall (which is needed for activating mechanosensory neurons), the signal transduction within Cho neurons, and the synaptic delay between Cho neurons and SONs. To apply the touch and the optogenetic stimulation of nociceptors at about the same time, the touch stimulation was applied 70 ms earlier than the optogenetic stimulation of nociceptors and lasted no less than 170 ms. For touch stimulus in Figure 1E, Figure 2A and Figure 3A, the strength was 10-28 mN. For other touch stimulations, the strength of touch was increased to ~28 mN.

When analyzing the response of A08n neurons, a spikelet with a steep rise followed by a slower recovery was counted as an A08n response. In addition, since the responses are temporally associated with stimuli, we repeatedly stimulated sensory neurons in each recording and calculated the average of A08n responses to minimize the influence of noise in the data analysis. The percent change in spikelet numbers was calculated. The spikelet number of A08n response to the activation of nociceptors alone was defined as N1, and

that to the combination of nociceptor activation and other experimental manipulations was defined as N2. The percent change was calculated as 100 x (N2 – N1) / N1. For recordings in Figure 1E, Figure 2A and Figure 3A, the response of A08n within 100 ms after the start of 470-nm light application was analyzed. For other A08n recordings, 470-nm light application was increased to 500 ms, and A08n responses within the 500 ms were analyzed.

Calcium imaging—To study the neural activity of Cho axon terminals in response to touch stimuli, GCaMP6f and CD4-tdTomato were co-expressed in Cho neurons. CD4-tdTomato serves as a reference signal for normalizing GCaMP6f signals. The imaging was performed on the same type of larval preparation as that used for electrophysiology; the larval preparation had intact PNS and CNS. The VNC was imaged using a Leica SP5 confocal system equipped with an HC Fluotar L 25x/NA0.95 W VISIR immersion objective lens (Leica). A resonate scanner was also used to achieve high scanning speed (8000 Hz). GCaMP6f was excited by a 488-nm laser, and CD4-tdTomato was excited by a 543-nm laser. Images were collected on single optical planes. Touch stimuli were applied in the same way as in the electrophysiological studies.

To test whether peristaltic muscle contractions activate Cho neurons, we performed calcium imaging of Cho neurons in larvae that were not dissected. The head and tail of a larva was pinned on Sylgard-coated dish. GCaMP6f and CD4-tdTomato were co-expressed in Cho neurons, which allowed us to use the CD4-tdTomato signal to calibrate the GCaMP6f signal during larval body movements. Scanning frequency was 1,000 Hz without resonate scanner. A 10x/NA0.40 DRY UV lens (Leica) was used. Time-lapse of a single-optical plane was acquired. The somas of the 5 lateral Cho neurons (lch5) were imagined. During imaging, larva moved its body periodically. GCaMP6f signals between moving phase and resting phase were compared and analyzed.

Imaging $GABA_BR1$-GFSTF in C4da axon terminals—Third instar larvae were dissected to expose the CNS. After fixation in 4% formaldehyde for 15~20 min, the samples were imaged with a Leica SP8 confocal system. A 63x/NA1.40 CS2 oil lens (Leica) was used. $GABA_BR1$-GFSTF are endogenous $GABA_BR1$s fused to EGFP. *ppk*-CD4-tdTomato, in which CD4-tdTomato is expressed by the *ppk* promoter, marks the C4da neurons. EGFP and CD4-tdTomato were excited by a 488-nm and 543-nm lasers, respectively. The wavelength range of each channel of signal acquisition was set to minimize potential bleed-through between the two channels. Moreover, fluorescent signals of EGFP and CD4-tdTomato were collected sequentially to avoid cross-talks between the two channels.

Evans blue staining—Evans blue staining was used to assess whether the touch stimuli that we delivered with the piezoelectric actuator damaged the tissues on the body wall. The method was modified from that in a previous report[24]. The larval body walls were incubated in cold 0.03 mg/ml Evans blue dye in 1x phosphate-buffered saline (PBS) for about 45 min. Then larvae samples were washed with cold 1x PBS for 3 times (10 min each). After washing, larvae samples were fixed in 4% formaldehyde for 15 min and mounted before bright-field imaging.

QUANTIFICATION AND STATISTICAL ANALYSIS

Prism 9 was used for statistical analysis. The type of statistical test used in each experiment is indicated in figure legends. Sample numbers are indicated in figures. P values are represented by asterisks: *: $p < 0.05$, **: $p < 0.01$, and ***: $p < 0.001$.

Supplementary Material

Refer to Web version on PubMed Central for supplementary material.

ACKNOWLEDGMENTS

We thank Dr. Dao-Qi Zhang for helping with setting up the patch-clamping recording, Dr. Wei Zhang for sharing information on piezoelectric actuator, Drs. Atit Patel and Dan Cox for advices on the heat-plate assay, Drs. Bo Duan, Dao-Qi Zhang, and members of the Ye lab for critical comments on an earlier version of this manuscript. This research was supported by National Institutes of Health (NIH) to B.Y. (R01NS104299) and National Natural Science Foundation of China to L.Y. (31571087). *Drosophila* Stocks from the Bloomington *Drosophila* Stock Center (NIH P40OD018537) were used in this study. The content is solely the responsibility of the authors and does not necessarily represent the official views of the NIH.

REFERENCES

1. Ma Q (2010). Labeled lines meet and talk: population coding of somatic sensations. The Journal of clinical investigation 120, 3773–3778. 10.1172/JCI43426. [PubMed: 21041959]
2. Auvray M (2019). Multisensory and spatial processes in sensory substitution. Restor Neurol Neurosci 37, 609–619. 10.3233/rnn-190950. [PubMed: 31796711]
3. Lloyd-Esenkaya T, Lloyd-Esenkaya V, O'Neill E, and Proulx MJ (2020). Multisensory inclusive design with sensory substitution. Cogn Res Princ Implic 5, 37. 10.1186/s41235-020-00240-7. [PubMed: 32770416]
4. Chizh BA, Dickenson AH, and Wnendt S (1999). The race to control pain: more participants, more targets. Trends Pharmacol Sci 20, 354–357. 10.1016/s0165-6147(99)01378-4. [PubMed: 10462755]
5. Driver J, and Noesselt T (2008). Multisensory interplay reveals crossmodal influences on 'sensory-specific' brain regions, neural responses, and judgments. Neuron 57, 11–23. 10.1016/j.neuron.2007.12.013. [PubMed: 18184561]
6. Tracey WD Jr., Wilson RI, Laurent G, and Benzer S (2003). painless, a Drosophila gene essential for nociception. Cell 113, 261–273. [PubMed: 12705873]
7. Hwang RY, Zhong L, Xu Y, Johnson T, Zhang F, Deisseroth K, and Tracey WD (2007). Nociceptive neurons protect Drosophila larvae from parasitoid wasps. Curr Biol 17, 2105–2116. 10.1016/j.cub.2007.11.029. [PubMed: 18060782]
8. Zhong L, Hwang RY, and Tracey WD (2010). Pickpocket Is a DEG/ENaC Protein Required for Mechanical Nociception in Drosophila Larvae. Current Biology 20, 429–434. [PubMed: 20171104]
9. Chin MR, and Tracey WD Jr. (2017). Nociceptive Circuits: Can't Escape Detection. Curr Biol 27, R796–R798. 10.1016/j.cub.2017.07.031. [PubMed: 28829963]
10. Zhang W, Yan Z, Jan LY, and Jan YN (2013). Sound response mediated by the TRP channels NOMPC, NANCHUNG, and INACTIVE in chordotonal organs of Drosophila larvae. Proceedings of the National Academy of Sciences of the United States of America 110, 13612–13617. 10.1073/pnas.1312477110. [PubMed: 23898199]
11. Yan Z, Zhang W, He Y, Gorczyca D, Xiang Y, Cheng LE, Meltzer S, Jan LY, and Jan YN (2013). Drosophila NOMPC is a mechanotransduction channel subunit for gentle-touch sensation. Nature 493, 221–225. 10.1038/nature11685. [PubMed: 23222543]
12. Ohyama T, Schneider-Mizell CM, Fetter RD, Aleman JV, Franconville R, Rivera-Alba M, Mensh BD, Branson KM, Simpson JH, Truman JW, et al. (2015). A multilevel multimodal circuit enhances action selection in Drosophila. Nature 520, 633–639. 10.1038/nature14297. [PubMed: 25896325]

13. Govorunova EG, Sineshchekov OA, Janz R, Liu XQ, and Spudich JL (2015). Natural light-gated anion channels: A family of microbial rhodopsins for advanced optogenetics. Science 349, 647–650. 10.1126/science.aaa7484. [PubMed: 26113638]

14. Mohammad F, Stewart JC, Ott S, Chlebikova K, Chua JY, Koh TW, Ho J, and Claridge-Chang A (2017). Optogenetic inhibition of behavior with anion channelrhodopsins. Nature methods 14, 271–274. 10.1038/nmeth.4148. [PubMed: 28114289]

15. Hu Y, Wang C, Yang L, Pan G, Liu H, Yu G, and Ye B (2020). A Neural Basis for Categorizing Sensory Stimuli to Enhance Decision Accuracy. Curr Biol 30, 4896–4909. 10.1016/j.cub.2020.09.045. [PubMed: 33065003]

16. Shearin HK, Dvarishkis AR, Kozeluh CD, and Stowers RS (2013). Expansion of the gateway multisite recombination cloning toolkit. PLoS One 8, e77724. 10.1371/journal.pone.0077724. [PubMed: 24204935]

17. Burgos A, Honjo K, Ohyama T, Qian CS, Shin GJ, Gohl DM, Silies M, Tracey WD, Zlatic M, Cardona A, and Grueber WB (2018). Nociceptive interneurons control modular motor pathways to promote escape behavior in Drosophila. eLife 7. 10.7554/eLife.26016.

18. Kaneko T, Macara AM, Li R, Hu Y, Iwasaki K, Dunnings Z, Firestone E, Horvatic S, Guntur A, Shafer OT, et al. (2017). Serotonergic Modulation Enables Pathway-Specific Plasticity in a Developing Sensory Circuit in Drosophila. Neuron 95, 623–638 e624. 10.1016/j.neuron.2017.06.034. [PubMed: 28712652]

19. Takagi S, Cocanougher BT, Niki S, Miyamoto D, Kohsaka H, Kazama H, Fetter RD, Truman JW, Zlatic M, Cardona A, and Nose A (2017). Divergent Connectivity of Homologous Command-like Neurons Mediates Segment-Specific Touch Responses in Drosophila. Neuron 96, 1373–1387. 10.1016/j.neuron.2017.10.030. [PubMed: 29198754]

20. Vogelstein JT, Park Y, Ohyama T, Kerr RA, Truman JW, Priebe CE, and Zlatic M (2014). Discovery of brainwide neural-behavioral maps via multiscale unsupervised structure learning. Science (New York, N.Y 344, 386–392. 10.1126/science.1250298. [PubMed: 24674869]

21. Yoshino J, Morikawa RK, Hasegawa E, and Emoto K (2017). Neural Circuitry that Evokes Escape Behavior upon Activation of Nociceptive Sensory Neurons in Drosophila Larvae. Current Biology 27, 2499–2504. 10.1016/j.cub.2017.06.068. [PubMed: 28803873]

22. Gerhard S, Andrade I, Fetterig RD, Cardona A, and Schneider-Mizell CM (2017). Conserved neural circuit structure across Drosophila larval development revealed by comparative connectomics. eLife 6. 10.7554/eLife.29089.

23. Hu Y, Wang Z, Liu T, and Zhang W (2019). Piezo-like Gene Regulates Locomotion in Drosophila Larvae. Cell Rep 26, 1369–1377 e1364. 10.1016/j.celrep.2019.01.055. [PubMed: 30726723]

24. van der Plas MC, Pilgram GS, de Jong AW, Bansraj MR, Fradkin LG, and Noordermeer JN (2007). Drosophila Dystrophin is required for integrity of the musculature. Mechanisms of development 124, 617–630. 10.1016/j.mod.2007.04.003. [PubMed: 17543506]

25. Michalikova M, Remme MWH, Schmitz D, Schreiber S, and Kempter R (2019). Spikelets in pyramidal neurons: generating mechanisms, distinguishing properties, and functional implications. Rev Neurosci 31, 101–119. 10.1515/revneuro-2019-0044. [PubMed: 31437125]

26. Epsztein J, Lee AK, Chorev E, and Brecht M (2010). Impact of spikelets on hippocampal CA1 pyramidal cell activity during spatial exploration. Science (New York, N. Y 327, 474–477. 10.1126/science.1182773. [PubMed: 20093475]

27. Hu C, Petersen M, Hoyer N, Spitzweck B, Tenedini F, Wang D, Gruschka A, Burchardt LS, Szpotowicz E, Schweizer M, et al. (2017). Sensory integration and neuromodulatory feedback facilitate Drosophila mechanonociceptive behavior. Nat Neurosci 20, 1085–1095. 10.1038/nn.4580. [PubMed: 28604684]

28. Klapoetke NC, Murata Y, Kim SS, Pulver SR, Birdsey-Benson A, Cho YK, Morimoto TK, Chuong AS, Carpenter EJ, Tian Z, et al. (2014). Independent optical excitation of distinct neural populations. Nature methods 11, 330–346. 10.1038/nmeth.2836.

29. Yao ZP, Macara AM, Lelito KR, Minosyan TY, and Shafer OT (2012). Analysis of functional neuronal connectivity in the Drosophila brain. Journal of neurophysiology 108.

30. Hosie AM, Aronstein K, Sattelle DB, and ffrench-Constant RH (1997). Molecular biology of insect neuronal GABA receptors. Trends in neurosciences 20, 570–503. [PubMed: 9416670]

31. Tuthill JC, and Wilson RI (2016). Parallel Transformation of Tactile Signals in Central Circuits of Drosophila. Cell 164, 1046–1059. 10.1016/j.cell.2016.01.014. [PubMed: 26919434]
32. Rohrbough J, and Broadie K (2002). Electrophysiological analysis of synaptic transmission in central neurons of Drosophila larvae. Journal of neurophysiology 88, 847–860. 10.1152/jn.2002.88.2.847. [PubMed: 12163536]
33. Nagarkar-Jaiswal S, Lee PT, Campbell ME, Chen K, Anguiano-Zarate S, Gutierrez MC, Busby T, Lin WW, He Y, Schulze KL, et al. (2015). A library of MiMICs allows tagging of genes and reversible, spatial and temporal knockdown of proteins in Drosophila. eLife 4. 10.7554/eLife.05338.
34. Perkins LA, Holderbaum L, Tao R, Hu YH, Sopko R, McCall K, Donghui YZ, Flockhart I, Binari R, Shim HS, et al. (2015). The Transgenic RNAi Project at Harvard Medical School: Resources and Validation. Genetics 201, 843–U868. 10.1534/genetics.115.180208. [PubMed: 26320097]
35. Fushiki A, Kohsaka H, and Nose A (2013). Role of sensory experience in functional development of Drosophila motor circuits. PLoS One 8, e62199. 10.1371/journal.pone.0062199. [PubMed: 23620812]
36. Hu Y, Ferrario CR, Maitland AD, Ionides RB, Ghimire A, Watson B, Iwasaki K, White H, Xi Y, Zhou J, and Ye B (2022). *LabGym*: quantification of user-defined animal behaviors using learning-based holistic assessment. bioRxiv. 10.1101/2022.02.17.480911.
37. Melzack R, and Wall PD (1965). Pain mechanisms: a new theory. Science (New York, N.Y 150, 971–979. 10.1126/science.150.3699.971. [PubMed: 5320816]
38. Dickenson AH (2002). Gate control theory of pain stands the test of time. Br J Anaesth 88, 755–757. 10.1093/bja/88.6.755. [PubMed: 12173188]
39. Jovanic T, Schneider-Mizell CM, Shao M, Masson JB, Denisov G, Fetter RD, Mensh BD, Truman JW, Cardona A, and Zlatic M (2016). Competitive Disinhibition Mediates Behavioral Choice and Sequences in Drosophila. Cell 167, 858–870 e819. 10.1016/j.cell.2016.09.009. [PubMed: 27720450]
40. Cheng LE, Song W, Looger LL, Jan LY, and Jan YN (2010). The role of the TRP channel NompC in Drosophila larval and adult locomotion. Neuron 67, 373–380. 10.1016/j.neuron.2010.07.004. [PubMed: 20696376]
41. Mendes CS, Bartos I, Akay T, Marka S, and Mann RS (2013). Quantification of gait parameters in freely walking wild type and sensory deprived Drosophila melanogaster. eLife 2, e00231. 10.7554/eLife.00231. [PubMed: 23326642]
42. Wu H, Zhang GA, Zeng S, and Lin KC (2009). Extraction of allyl isothiocyanate from horseradish (Armoracia rusticana) and its fumigant insecticidal activity on four stored-product pests of paddy. Pest Manag Sci 65, 1003–1008. 10.1002/ps.1786. [PubMed: 19459178]
43. Xiang Y, Yuan Q, Vogt N, Looger LL, Jan LY, and Jan YN (2010). Light-avoidance-mediating photoreceptors tile the Drosophila larval body wall. Nature 468, 921–926. 10.1038/nature09576. [PubMed: 21068723]
44. Jenett A, Rubin GM, Ngo TT, Shepherd D, Murphy C, Dionne H, Pfeiffer BD, Cavallaro A, Hall D, Jeter J, et al. (2012). A GAL4-driver line resource for Drosophila neurobiology. Cell Rep 2, 991–1001. 10.1016/j.celrep.2012.09.011. [PubMed: 23063364]
45. Sineshchekov OA, Govorunova EG, Li H, and Spudich JL (2015). Gating mechanisms of a natural anion channelrhodopsin. Proceedings of the National Academy of Sciences of the United States of America 112, 14236–14241. 10.1073/pnas.1513602112. [PubMed: 26578767]
46. Nagel G, Szellas T, Huhn W, Kateriya S, Adeishvili N, Berthold P, Ollig D, Hegemann P, and Bamberg E (2003). Channelrhodopsin-2, a directly light-gated cation-selective membrane channel. Proceedings of the National Academy of Sciences of the United States of America 100, 13940–13945. 10.1073/pnas.1936192100. [PubMed: 14615590]
47. Chater TE, Henley JM, Brown JT, and Randall AD (2010). Voltage- and temperature-dependent gating of heterologously expressed channelrhodopsin-2. J Neurosci Methods 193, 7–13. 10.1016/j.jneumeth.2010.07.033. [PubMed: 20691205]
48. Patel AA, and Cox DN (2017). Behavioral and Functional Assays for Investigating Mechanisms of Noxious Cold Detection and Multimodal Sensory Processing in Drosophila Larvae. Bio Protoc 7. 10.21769/BioProtoc.2388.

49. Grueber WB, Ye B, Yang CH, Younger S, Borden K, Jan LY, and Jan YN (2007). Projections of Drosophila multidendritic neurons in the central nervous system: links with peripheral dendrite morphology. Development 134, 55–64. 10.1242/dev.02666. [PubMed: 17164414]

50. Han C, Jan LY, and Jan YN (2011). Enhancer-driven membrane markers for analysis of nonautonomous mechanisms reveal neuron-glia interactions in Drosophila. Proceedings of the National Academy of Sciences of the United States of America 108, 9673–9678. [PubMed: 21606367]

51. Schindelin J, Arganda-Carreras I, Frise E, Kaynig V, Longair M, Pietzsch T, Preibisch S, Rueden C, Saalfeld S, Schmid B, et al. (2012). Fiji: an open-source platform for biological-image analysis. Nature methods 9, 676–682. 10.1038/Nmeth.2019. [PubMed: 22743772]

Highlights

- Gentle mechanical stimuli inhibit nociceptive responses in *Drosophila* larvae.
- The cross-modal inhibition filters out only weak nociceptive inputs.
- Mechanosensory neurons inhibit A08n neurons in the nociceptive pathway.
- The cross-modal inhibition is mediated by $GABA_B$ receptors in nociceptors.

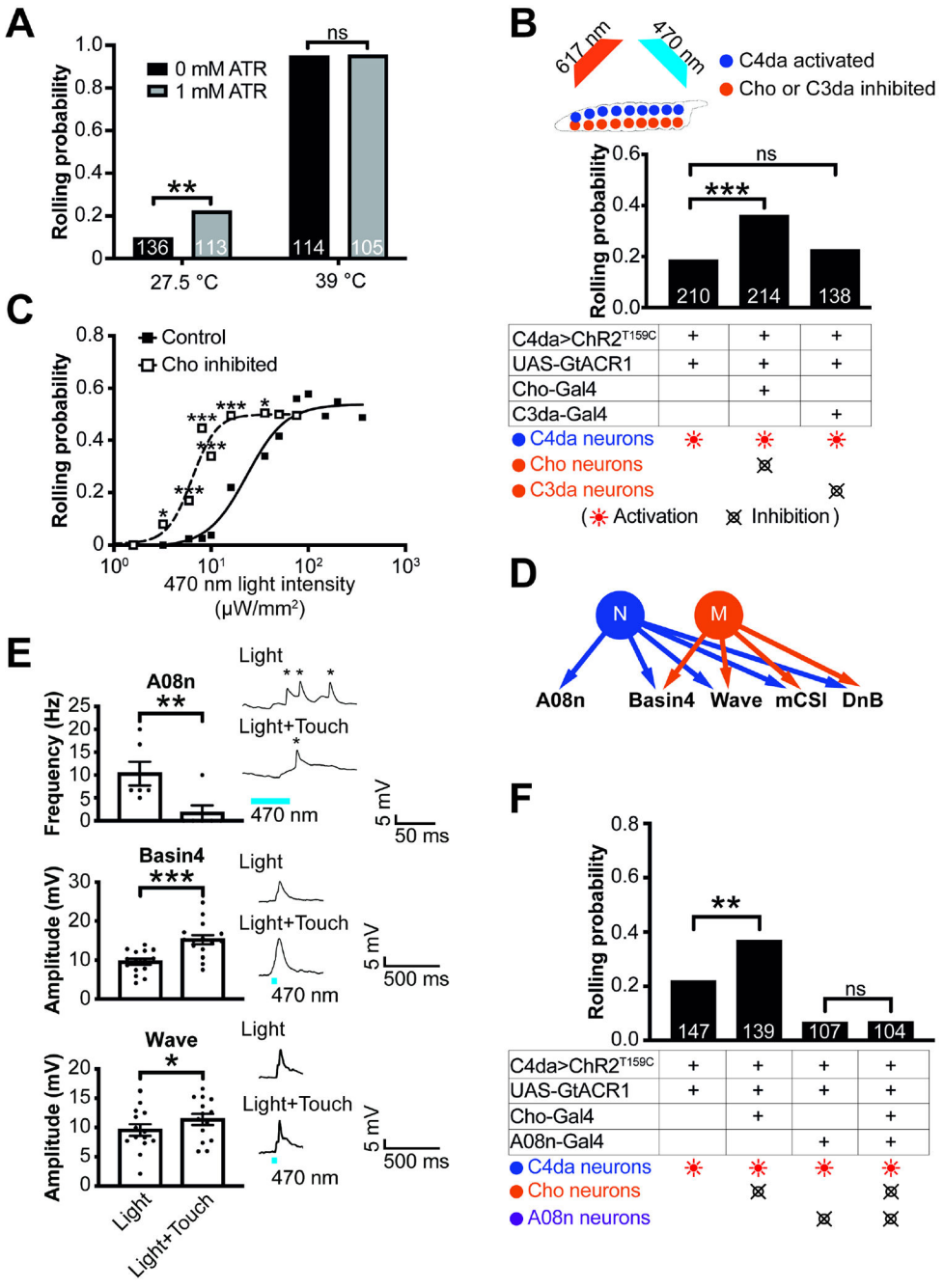

Figure 1. The low-threshold mechanosensory neuron Cho inhibits the nociceptor-specific SON A08n to modulate nociceptive behavior.

(A) Inhibition of Cho neurons via GtACR1 increases the probability of nociceptive rolling in larvae at a low (27.5°C), but not a high (39°C), temperature. Larvae expressing GtACR1 in their Cho neurons were placed on a pre-heated plate and illuminated with 617-nm light to activate GtACR1 for 1 min, during which the rolling behavior was scored. Since GtACR1 requires all-trans-retinal (ATR) for its activation, larvae reared on food that lacked ATR serve as the negative control for Cho inhibition. Chi-square with post-hoc Fisher's exact test. Sample numbers are indicated in the bars. **: $p < 0.01$; ns: $p > 0.05$.

(**B**) Inhibition of Cho neurons increases the probability of larval rolling elicited by nociceptor activation. Top, a cartoon depicting the optogenetic scheme of activating C4da nociceptors. ChR2^{T159C} was expressed in C4da nociceptors for optogenetic activation by 470-nm light (16 μW/mm^2), and GtACR1 was expressed in either Cho or C3da mechanosensory neurons (symbolized as orange dots) for optogenetic inhibition by 617-nm light. Bottom, inhibition of Cho, but not C3da, increased nociceptor-elicited rolling. Chi-square with post-hoc Fisher's exact test. Sample numbers are indicated in the bars. ***: $p < 0.001$.

(**C**) Inhibition of Cho neurons sensitizes larvae to nociceptor activation. The probability of larval rolling under different intensities of optogenetic stimulation of C4da nociceptors. Each square represents a group of 56-116 larvae. The curves were fit with sigmoidal non-linear regression (R^2: control, 0.97; Cho inhibited, 0.96). The probability of rolling began to rise at about 10^1 μW/mm^2 and plateaued at about 10^2 μW/mm^2. Inhibition of Cho neurons (via GtACR1) shifted the stimulus-response curve to the left, demonstrating that larvae became more sensitive to lower activity of nociceptors.

(**D**) A schematic showing that while most SONs receive input from both nociceptors (N) and mechanosensory neurons (M), A08n only receives input from nociceptors. Basin4, Wave, and DnB are shown as representative multisensory SONs. This connectivity makes A08n a unique SON for studying synaptic and circuit mechanisms underlying cross-modal modulation.

(**E**) Gentle touches suppress A08n's response, but enhance the responses of Basin-4 and Wave, to nociceptor activation. C4da nociceptors expressing ChR2^{T159C} were activated by 470-nm light (0.5, 2, and 2 μW/mm^2 for A08n, Basin-4, and Wave, respectively) for 50 ms (blue bars under the traces). Gentle touch (10-16 mN) on the body wall was applied with a piezoelectric actuator. A08n responded to C4da activation with graded depolarization superposed with multiple spikelets (each marked by an asterisk above it), whereas Basin-4 and Wave responded with a single peak of graded depolarization. We calculated the frequency of A08n responses within a 100-ms time-window from the onset of the blue light. The peak amplitudes of Basin-4 and Wave responses were measured. Paired Student's t-test. Sample numbers are indicated in the bars. *: $p < 0.05$, **: $p < 0.01$, and ***: $p < 0.001$.

(**F**) The modulation of nociceptive rolling by Cho neurons requires A08n activity. Inhibition of Cho enhanced nociceptor-induced rolling when A08n activity was intact (bar 1 and 2), but not when A08n was inhibited (bar 3 and 4). As previously reported[15,18,27], inhibition of A08n reduced nociceptor rolling (bar 1 and 3). Chi-square with post-hoc Fisher's exact test. Sample numbers are indicated in the bars. **: $p < 0.01$, ns: $p > 0.05$.

See also Figure S1, Figure S2, Figure S4, and Video S1.

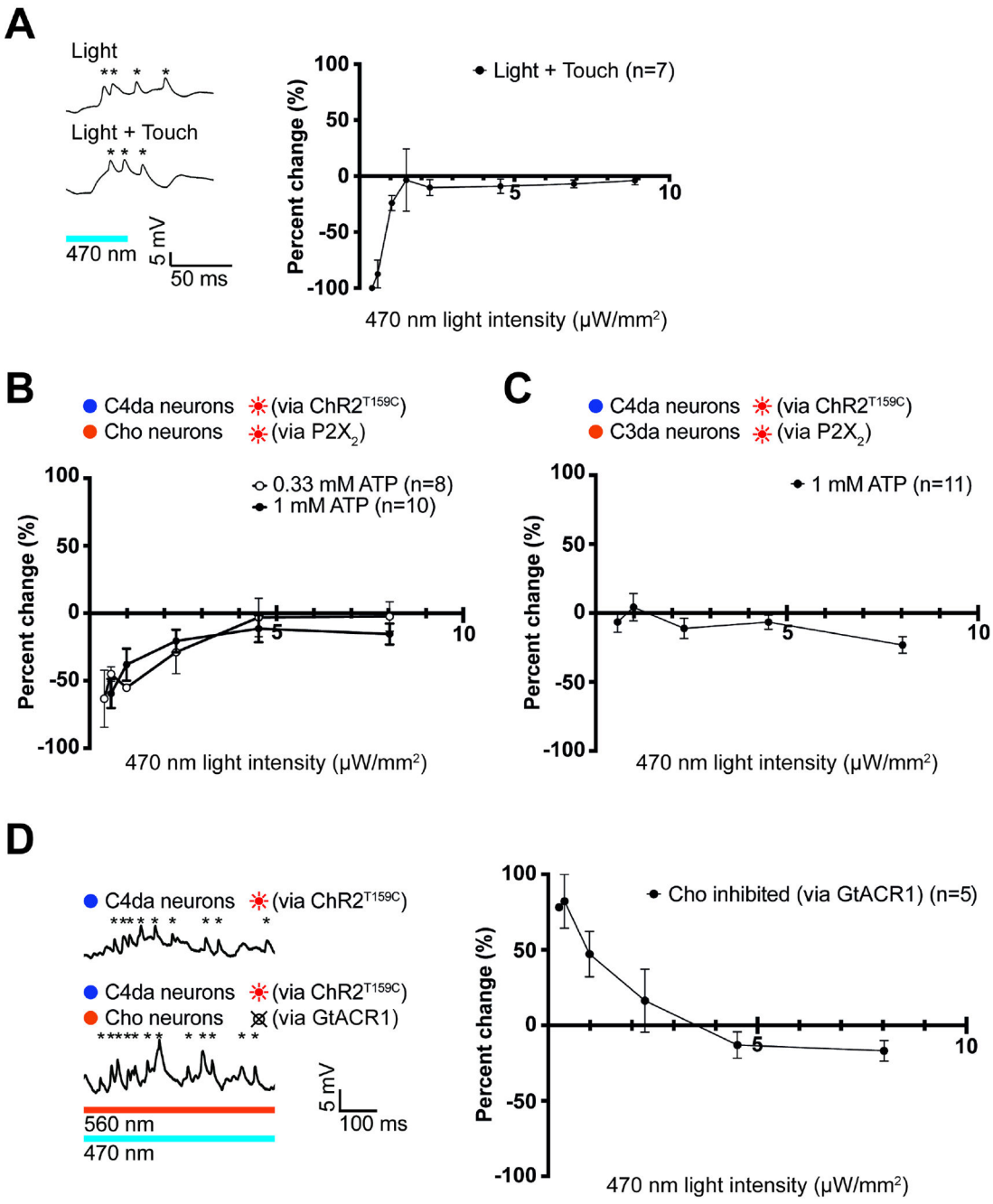

Figure 2. Cho neurons selectively suppress the weak inputs from nociceptors.

(**A**) Gentle touch selectively inhibits A08n's electrophysiological responses elicited by weak activation of nociceptors. C4da nociceptors expressing ChR2^{T159C} were activated by 470-nm light (50 ms duration) at intensities ranging from 0.40 to 8.89 μW/mm^2. The touch stimulus (10 mN) was delivered by a piezoelectric actuator. The spikelets are marked by asterisks above them. For brief optogenetic activations of C4da nociceptors (50 ms), A08n responses within a 100-ms time-window from the onset of the blue light were counted, and the spikelet frequency was calculated to obtain the percent change caused by the touch stimulus. A08n's response was attenuated at low intensities of C4da activation (0.40 to 1.04

μW/mm^2) but not at higher intensities. Error bars show mean ± SEM. The number of cells recorded are shown in the figures.

(**B-C**) Cho, but not C3da, mechanosensory neurons inhibits A08n's responses that are elicited by weak activation of nociceptors. Cho (B) or C3da (C) mechanosensory neurons expressing $P2X_2$ were activated by bath-application of ATP, whereas C4da nociceptors expressing ChR2^{T195C} were activated by 470-nm light at the indicated intensities. Activation of Cho (with 0.33 and 1 mM ATP) inhibited A08n responses to weak activation of C4da in a fashion similar to gentle touch (shown in panel A).

(**D**) Inhibition of Cho neurons increases A08n's responses elicited by weak activation of nociceptors. C4da nociceptors expressing ChR2^{T159C} were activated as above (blue bar). Cho neurons expressing GtACR1 were inhibited by 560-nm light (7.80 μW/mm^2, orange bar). At this intensity, 560-nm light did not activate A08n. 560-nm light was applied 250 ms earlier than the 470-nm blue light to ensure that GtACR1 was activated during the entire period of C4da activation. Inhibition of Cho dramatically enhanced A08n's response to C4da activation in the low intensity range of 470-nm light. For prolonged optogenetic stimulations (500 ms), A08n responses during the entire period was analyzed. The spikelets are marked by asterisks above them.

See also Figure S1 and Figure S2.

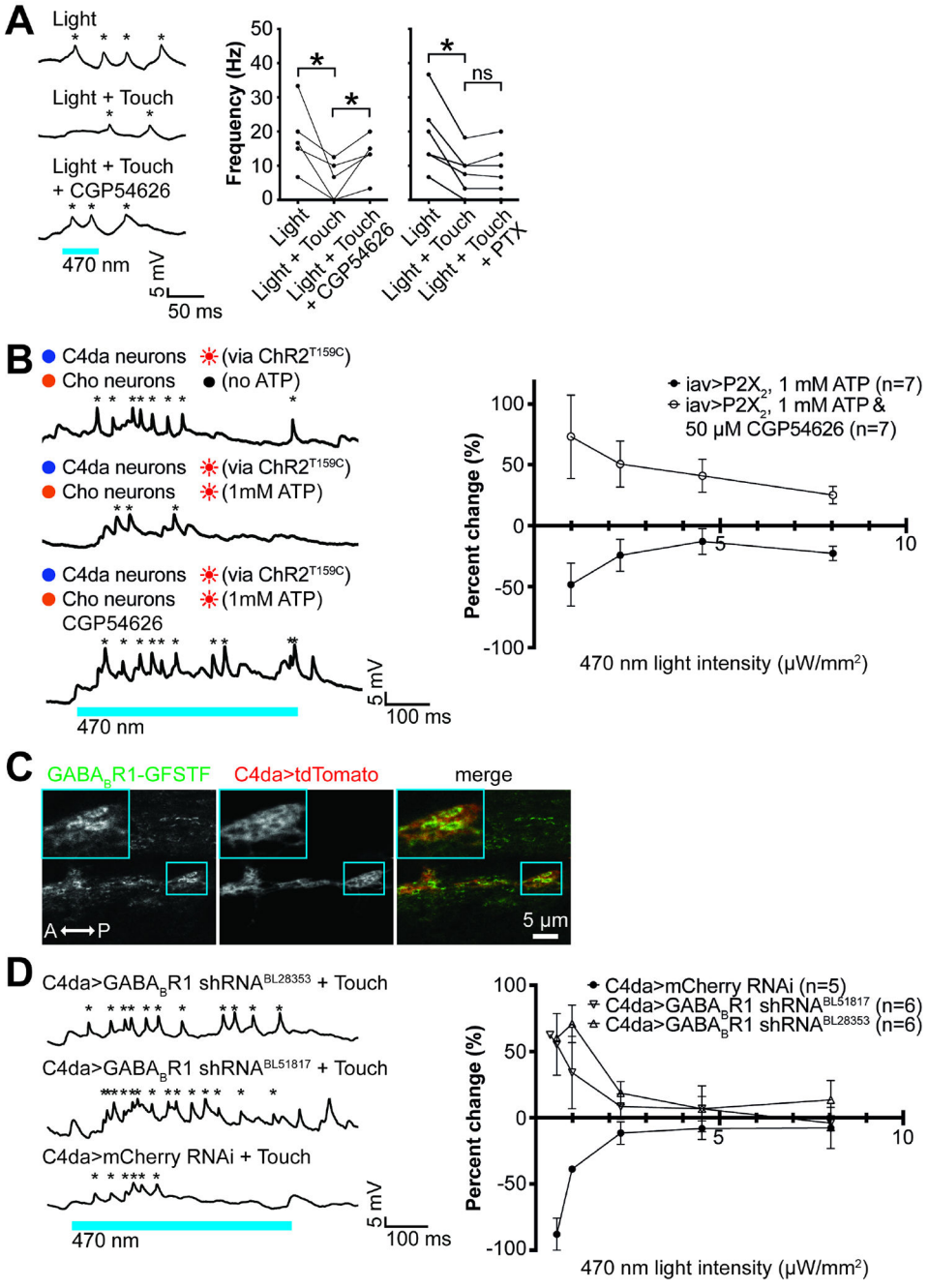

Figure 3. The cross-modal gating of nociceptive inputs is mediated by the $GABA_B$ receptor $GABA_BR1$.

(**A**) The $GABA_B$ receptor antagonist CGP54626 (50 μM), but not the $GABA_A$ antagonist PTX (10 μM), diminishes the inhibition of nociceptor-elicited A08n responses by touch. A08n's response frequency was quantified. C4da nociceptors expressing $ChR2^{T159C}$ were activated by 470-nm light (blue bar) for 50 ms. One-way ANOVA with Tukey post-hoc test. *: $p < 0.05$.

(**B**) $GABA_B$ receptor antagonist CGP54626 reverses the inhibition of A08n response by Cho neurons. Cho neurons expressing $P2X_2$ were activated by bath-application of 1 mM ATP,

and C4da nociceptors expressing ChR2^{T159C} were activated by 470-nm light (500 ms, blue bar). Cho activation reduced A08n's response to weak activation of C4da nociceptors, and CGP54626 reversed this inhibition.

(**C**) $GABA_BR1$ receptors are expressed in the axon terminals of C4da nociceptors. We used the MiMIC-RMCE line, $GABA_BR1$-GFSTF, to label $GABA_BR1$ receptors and *ppk*-tdTomato to mark C4da neurons. Images shown are from a single optic section from confocal imaging. Shown is the part of the VNC between the abdominal segment 4 (A4) and A5. $GABA_BR1$ receptors colocalized with C4da axon terminals.

(**D**) $GABA_BR1$ is required in C4da nociceptors for touch stimuli to inhibit A08n responses at weak activation of nociceptors. Knockdown of $GABA_BR1$ in C4da nociceptors with either shRNA^{BL28353} or shRNA^{BL51817} reversed the inhibition of A08n response to touch. C4da neurons expressing ChR2^{T159C} were activated by 470-nm light for 500 ms (blue bar). Touch stimuli (~28 mN) were delivered by a piezoelectric actuator 70 ms earlier than the 470-nm light. The effect of $GABA_BR1$ knockdown resembles that of the $GABA_B$ receptor antagonist CGP54626.

The spikelets are marked by asterisks above them.

See also Figure S1, Figure S2, and Figure S3.

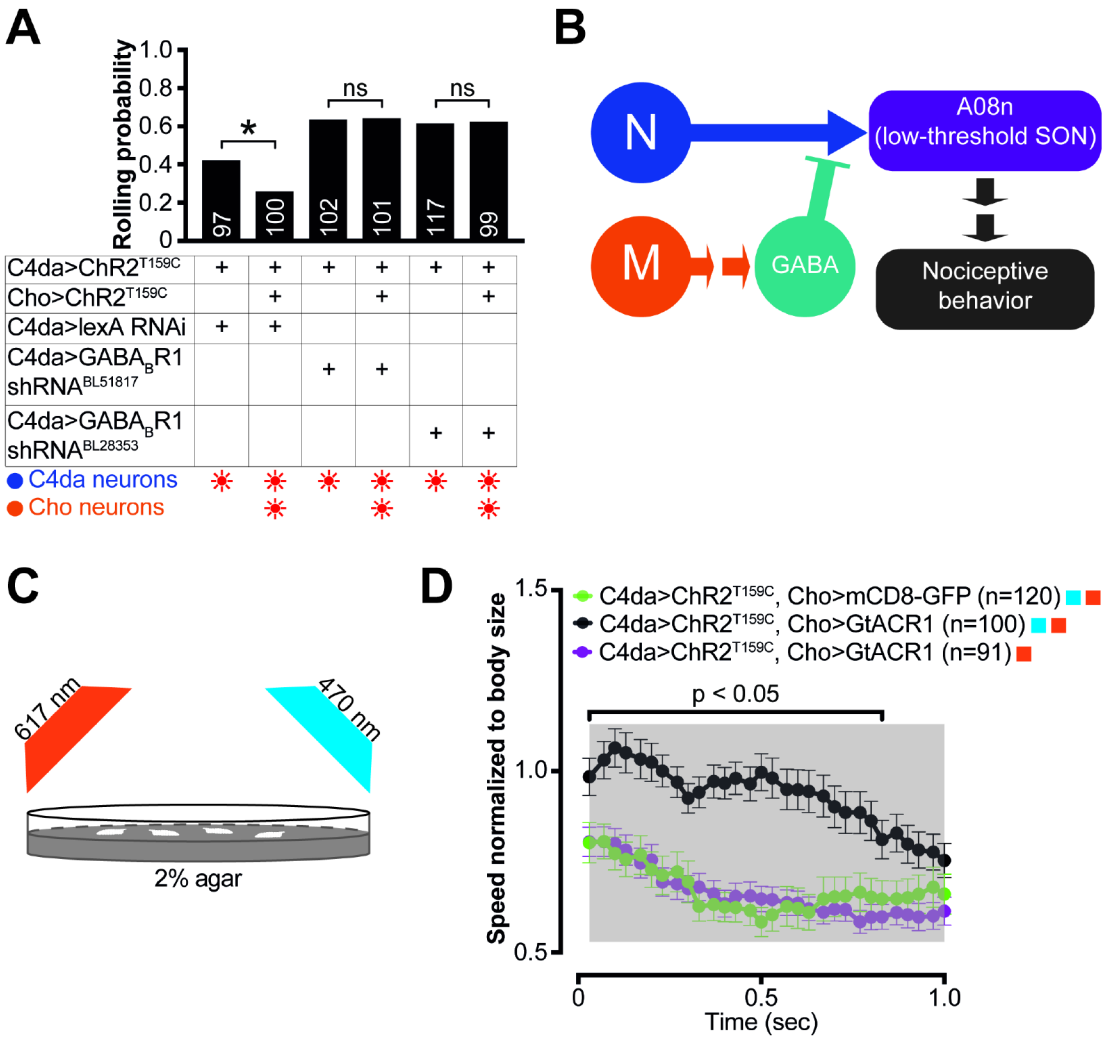

Figure 4. Nociceptor-elicited body movements attenuate nociceptive inputs.

(**A**) The Cho-mediated suppression of C4da-induced nociceptive rolling is abolished by the knockdown of $GABA_BR1$ receptors in C4da nociceptors. A shRNA against LexA was used as the negative control. Sample numbers are indicated in the bars. Chi-square with post-hoc Fisher's exact test. *: $p < 0.05$, ns: $p > 0.05$.

(**B**) A model of the circuit for the cross-modal inhibition of larval nociceptive pathway. The C4da nociceptors synapse on A08n. The Cho neurons modulate the C4da-to-A08n synapse via GABAergic neurons.

(**C**) A schematic drawing that shows the hard-agar assay for larval nociceptive behavior. Larvae expressing $ChR2^{T159C}$ in their C4da nociceptors also expressed either GFP or GtACR1 in their Cho neurons. $ChR2^{T159C}$ and GtACR1 were activated by 470-nm and 617-nm lights, respectively. The lights were on for 2 sec. Third-instar larvae were placed on the dry surface of hard agar (2%). Larval behavior were recorded by a video camera.

(**D**) Inhibition of Cho neurons increases the speed of nociceptor-elicited crawling. Larval behavior were analyzed with the software tool LabGym[36]. The y-axis is the speed normalized to the body size of the larva. The gray area indicates that the lights were

on during the period. Blue and orange squares indicate the application of 470-nm and 617-nm lights, respectively. Sample numbers are shown in the figure. Two-way ANOVA with post-hoc Dunnett test comparing the Cho inhibition group (black dots) with the group without Cho inhibition (green dots). Data points with $p < 0.05$ are indicated in the chart. See also Figure S3, Figure S4, and Video S1.

KEY RESOURCES TABLE

REAGENT or RESOURCE	SOURCE	IDENTIFIER
Experimental models: Organisms/strains		
Drosophila: UAS-GtACR1-YFP	Mohammad et al.[14]	N/A
Drosophila: LexAop2-GtACR1-YFP	Mohammad et al.[14]	N/A
Drosophila: MB120B-splitGAL4	Takagi et al.[19]	N/A
Drosophila: ppk-GAL4	Grueber et al.[49]	N/A
Drosophila: iav-GAL4	Bloomington *Drosophila* stock center	BDSC:52273
Drosophila: GMR82E12-GAL4	Bloomington *Drosophila* stock center	BDSC:40153
Drosophila: GMR83B04-GAL4	Bloomington *Drosophila* stock center	BDSC:41309
Drosophila: GMR82E12-LexA	Bloomington *Drosophila* stock center	BDSC:54417
Drosophila: GMR57F07-LexA	Bloomington *Drosophila* stock center	BDSC:54899
Drosophila: TrpA1-QF	Bloomington *Drosophila* stock center	BDSC:36345
Drosophila: iav-QF	Bloomington *Drosophila* stock center	BDSC:36347
Drosophila: UAS-CD4-tdGFP	Bloomington *Drosophila* stock center	BDSC:35836
Drosophila: UAS-mCD8-GFP	Bloomington *Drosophila* stock center	BDSC:32185; BDSC:32186
Drosophila: UAS-mCherry	Bloomington *Drosophila* stock center	BDSC:52267
Drosophila: UAS-ChR2-XXL	Bloomington *Drosophila* stock center	BDSC:58374
Drosophila: UAS-$P2X_2$	Yao et al.[29]	N/A
Drosophila: UAS-$GABA_BR1$ $shRNA^{BL28353}$	Bloomington *Drosophila* stock center	BDSC:28353
Drosophila: UAS-GABABR1 $shRNA^{BL51817}$	Bloomington *Drosophila* stock center	BDSC:51817
Drosophila: UAS-mCherry RNAi	Bloomington *Drosophila* stock center	BDSC:35785
Drosophila: UAS-LexA RNAi	Bloomington *Drosophila* stock center	BDSC:67945
Drosophila: LexAop2-mCherrry-HA	Bloomington *Drosophila* stock center	BDSC:52272
Drosophila: QUAS-$ChR2^{T159C}$-HA	Bloomington *Drosophila* stock center	BDSC:52260; BDSC:52259
Drosophila: $GABA_BR1$-GFSTF	Bloomington *Drosophila* stock center	BDSC:60522
Drosophila: ppk-CD4-tdTomato	Han et al.[50]	N/A
Software and algorithms		
Prism 9	Graphpad	N/A
ImageJ 1.53c (Fiji)	Schindelin et al.[51]	https://imagej.net/software/fiji/
Igor pro 6.3	WaveMetrics	https://www.wavemetrics.com
Leica Application Suite Advanced Fluorescence	Leica Microsystems	https://www.leica-microsystems.com/products/microscope-software/p/leica-las-x-ls/
Optical Power Monitor v1.1	Thorlabs	https://www.thorlabs.com/software_pages/ViewSoftwarePage.cfm?Code=OPM
LabGym (version 1.4)	Hu et al.[36]	https://github.com/umyelab/LabGym
ARDUINO 1.8.7	Arduino	https://www.arduino.cc